College of Engineering

Drexel E-Repository and Archive (iDEA)
http://idea.library.drexel.edu/

Drexel University Libraries
www.library.drexel.edu

The following item is made available as a courtesy to scholars by the author(s) and Drexel University Library and may contain materials and content, including computer code and tags, artwork, text, graphics, images, and illustrations (Material) which may be protected by copyright law. Unless otherwise noted, the Material is made available for non profit and educational purposes, such as research, teaching and private study. For these limited purposes, you may reproduce (print, download or make copies) the Material without prior permission. All copies must include any copyright notice originally included with the Material. **You must seek permission from the authors or copyright owners for all uses that are not allowed by fair use and other provisions of the U.S. Copyright Law.** The responsibility for making an independent legal assessment and securing any necessary permission rests with persons desiring to reproduce or use the Material.

Please direct questions to archives@drexel.edu

Self-exciting, self-sensing $PbZr_{0.53}Ti_{0.47}O_3/SiO_2$ piezoelectric microcantilevers with femtogram/Hertz sensitivity

Zuyan Shen, Wan Y. Shih,[a] and Wei-Heng Shih
Department of Materials Science and Engineering, Drexel University, Philadelphia, Pennsylvania 19104

(Received 27 March 2006; accepted 22 May 2006; published online 12 July 2006)

Piezoelectric microcantilever sensors (PEMSs) consisting of a piezoelectric layer bonded to a nonpiezoelectric layer offer the advantages of electrical self-actuation and self-detection. Here we report PEMSs 60–300 μm in length fabricated from 1.5-μm-thick sol-gel $PbZr_{0.53}Ti_{0.47}O_3$ (PZT) films with a 2 μm grain size, a dielectric constant of 1600, and a saturation polarization of 55 ± 5 $\mu C/cm^2$. The PEMSs exhibited up to four resonance peaks with quality factors Q ranging from 120 to 320. In humidity sensing tests, a PEMS with a 60×25 μm PZT/SiO_2 section and a 24×20 μm SiO_2 extension exhibited 1×10^{-15} g/Hz mass sensitivity, two orders of magnitude better than the sensitivity of the current PZT PEMS. © *2006 American Institute of Physics*. [DOI: 10.1063/1.2219994]

Microcantilever sensors have attracted considerable interest because of their capability for label-free biological detection.[1–12] As a sensor, receptors are immobilized on the cantilever surface. Binding of target biological or chemical agents to the receptors on the cantilever surface forces the cantilever bend[1] and its resonance frequency shift.[2–12] Detection of target analytes can be achieved by either measuring the cantilever tip displacement[1] or its resonance frequency shift.[2–12] Piezoelectric microcantilever sensors (PEMSs) are microcantilevers consisting of a piezoelectric layer, e.g., lead zirconate titanate (PZT) bonded to a nonpiezoelectric layer, e.g., SiO_2. Unlike silicon-based microcantilevers that require an external actuator for excitation[2,3] and an external optical system for detection,[1–3] PEMSs can electrically self-excite and self-detect. Applying an alternating current (ac) voltage across the piezoelectric layer causes the PEMSs to vibrate, which generates a measurable piezoelectric voltage across the piezoelectric layer that can be used to monitor PEMS resonance frequency shift.[4,5,7–12] Commercial ZnO-based PEMSs have been used for in-air vapor detection[13–16] by either monitoring bending[13,14] or by monitoring the resonance frequency shift.[14–16] PZT PEMSs due to their higher piezoelectric coefficients have been demonstrated for *in situ* biological detections[4,5,7,10,11] in addition to in-air chemical[12] and *ex situ* protein detection.[8,9] Current $300\times50\times3$ μm^3 ZnO PEMS and $150\times50\times2$ μm^3 PZT/Si_3N_4 PEMS exhibited a mass sensitivity of 10^{-11}–10^{-12} g/Hz for in-air trinitrotoluene (TNT) vapor detection[14,15] and 10^{-13} g/Hz for in-air *ex situ* protein detection,[8,9] respectively.

The objective of this study is to further increase the mass sensitivity of PEMSs to the level of femtogram/hertz by reducing the size of PEMSs through microfabrication and materials synthesis. Smaller cantilevers are known to exhibit better mass sensitivities: A 3.5 μm long silicon nanocantilever exhibited 10^{-21} g/Hz mass sensitivity in vacuum.[17] Further studies showed that the mass sensitivity $\Delta f/\Delta m$ of a cantilever of length L and width w was related to L and w as[18] $\Delta f/\Delta m \propto \nu_i^2/(L^3 w)$, where Δm and Δf denote the mass change and the corresponding resonance frequency shift, respectively, and ν_i^2 the dimensionless ith-mode eigenvalue. This indicates that reducing a cantilever's dimensions proportionally by a factor of α increases its mass sensitivity by a factor of α^{-4} and that use of a higher-mode resonance peak increases the mass sensitivity. The difficulty with a reduced cantilever's size is that the resonance peak heights quickly diminish, rendering the cantilever unsuitable for sensing. Strategies to improve a PEMS resonance peak height include amplifying the piezoelectric voltage and reducing the noise with a bridge circuit[19] or incorporating on the silicon substrate a piezoelectric patch of the same material and dimension as the PEMS,[20] and/or replacing the ZnO that offers piezoelectric coefficients in the range of $d_{31}=-4$ pm/V and $d_{33}=12.4$ pm/V,[21] with PZT. Most PZT films exhibit piezoelectric coefficients ranging from $d_{31}=-58$ pm/V (Ref. 20) to $d_{33}=190$–250 pm/V.[22,23] Although these values are much higher than those of ZnO, they are only about 20%–40% of those of the bulk commercial PZT,[24] due to interfacial diffusion and substrate pinning. As a result, it is challenging to achieve small PEMSs that can both self-excite and self-sense. A PZT layer with improved piezoelectric properties may help reduce the size of self-exciting and self-sensing PEMSs.

An earlier study[25] has shown that using a sol-gel procedure with ethylene glycol as solvent, one could achieve 1.5-μm-thick fully dense PZT films that exhibited an average grain size of 2 μm, a dielectric constant of 1600, and a saturation polarization of 55 ± 5 $\mu C/cm^2$ with a maximum applied electric field $E_{max}=600$ kV/cm, better than the typical dielectric constant (800–1000) and saturation polarization (20–40 $\mu C/cm^2$) of most PZT films.

In this study, we fabricated self-exciting and self-sensing PZT/SiO_2 PEMSs as small as 60 μm in length with a 24×20 μm^2 SiO_2 extension using PZT films obtained with the above sol-gel procedure. First, a 2-μm-thick low-stress SiO_2 layer was deposited on a 3 in. silicon wafer by steam oxidation at 850 °C. A 1500-Å-thick platinum bottom electrode with a 400-Å-thick TiO_2 bonding layer was then deposited by Radiant Technologies (Albuquerque, NM). A 1.5-μm-thick PZT layer was then deposited. On the PZT layer, 400 Å titanium followed by 1000-Å-thick platinum and 5000-Å-thick nickel was deposited by e-gun evaporation (Semicore Equipment, Livermore, CA) and patterned by a photolithographic lift-off process. The nickel layer was used as the hard mask in the dry etching process. The PZT layer

[a]Electronic mail: shihwy@drexel.edu

 © 2006 American Institute of Physics
Downloaded 25 Jul 2006 to 129.25.131.237. Redistribution subject to AIP license or copyright, see http://apl.aip.org/apl/copyright.jsp

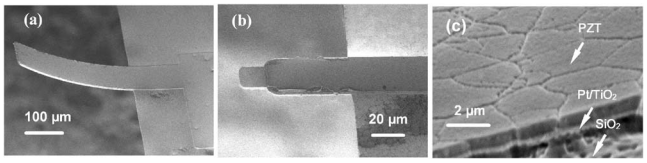

FIG. 1. (a) A SEM photograph of a 300×70 μm PZT/SiO_2 PEMS (PEMS-1), (b) that of a 60×25 μm PZT/SiO_2 PEMS with 24×20 μm SiO_2 extension (PEMS-2), and (c) that of the top surface of an ICP-etched PZT layer.

and the TiO_2/Pt bottom electrode were patterned by inductively coupled plasma (ICP) dry etching (Applied Materials Cluster Tool, Santa Clara, CA). The underside of the silicon wafer was removed by backside KOH wet etching. The SiO_2 membrane was etched by reactive ion etching (RIE) (P5000 MERIE, Applied Materials, Santa Clara, CA) to release the PEMSs. All PEMSs had a 1.5-μm-thick PZT layer and a 2.0-μm-thick SiO_2 layer. Figures 1(a) and 1(b) respectively show the scanning electron microscopy (SEM) (LEO 440, Carl Zeiss Worldwide, Germany) micrograph of a 300×70 μm PZT/SiO_2 PEMS (PEMS-1) and that of a 60×25 μm PZT/SiO_2 PEMS with a 24×20 μm SiO_2 extension (PEMS-2). Clearly, the PZT layer was dense with a smooth surface. Figure 1(c) shows a SEM micrograph of an ICP-etched PZT surface revealing that the PZT layer had an average grain size of about 2 μm, larger than the PZT thickness. This indicates that the PZT layer was well sintered, consistent with the earlier results that the PZT film could withstand an electric field of 600 kV/cm.

Both PEMS-1 and PEMS-2 exhibited a relative dielectric constant of 1500 at 10 kHz as measured by an HP 4275A multifrequency *LCR* meter, consistent with the pre-microfabrication value, 1600, and indicated that the microfabrication process had little damage to the PZT layers. The PEMSs were "poled" at room temperature by a dc bias voltage of 15 V (100 kV/cm) for 30 min during the impedance spectrum scan (4294A, Agilent, Palo Alto, CA). In what follows, all resonance spectra were taken with a 15 V dc bias. The resonance frequency spectrum of PEMS-1 is shown in Fig. 2. As can be seen, PEMS-1 exhibited four resonance peaks at 17.9, 106.2, 305.7, and 608.6 kHz, corresponding to the first four flexural vibration modes. The calculated first four flexural resonance frequencies using a method for PEMSs of uniform thickness[18] were 17.8, 110.4, 307.9, and 612.3 kHz, as marked by the vertical dashed lines. For PEMS-2, we observed only the first peak at 408 kHz, as shown in Fig. 3(a) by the dashed-dotted line at 31.2% relative humidity, which was in agreement with the theoretical

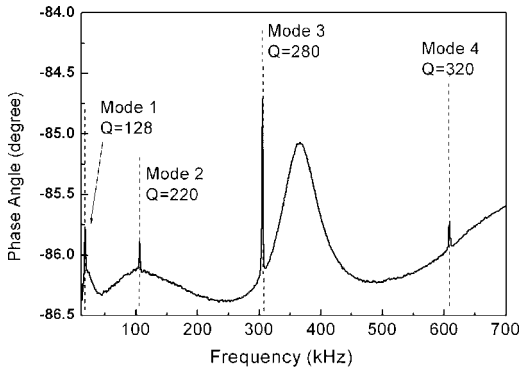

FIG. 2. Resonance spectrum of a 300×70 μm PZT/SiO_2 PEMS (PEMS-1). The vertical dashed lines indicate the theoretical resonance frequencies.

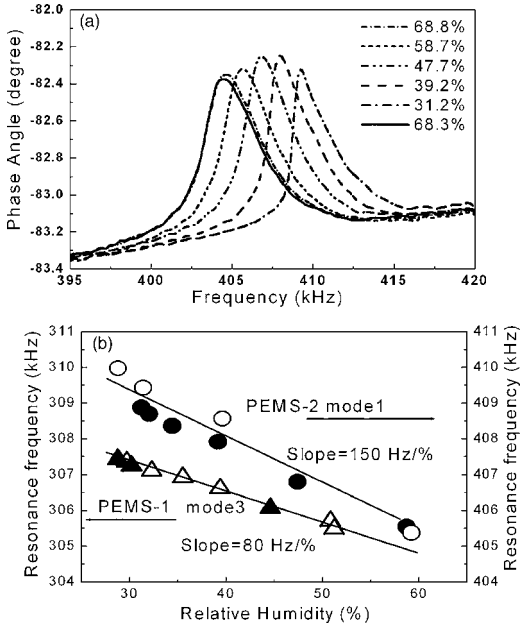

FIG. 3. (a) The first-mode resonance spectra of PEMS-2 at various humidity levels and (b) resonance frequency vs relative humidity. Open (filled) triangles and open (filled) circles denote the humidity downsweep (upsweep) for the third-mode resonance peak of PEMS-1 and the first-mode resonance peak of PEMS-2, respectively.

first-peak resonance frequency, 412 kHz, obtained using a model for a two-sectioned PEMS (Ref. 30) and marked by the vertical dashed line. Note that all the resonance peaks exhibited high quality factors Q ranging from 120 to 320, where Q was defined as the ratio of the resonance frequency relative to the resonance peak width at half the peak height.

For mass sensitivity determination, the PEMSs were placed in a closed probe station (Micromanipulator, Carson City, NV) with an initial relative humidity of 68.3% and temperature of 21.6 °C. The humidity level inside the chamber was reduced by flowing dry nitrogen. Different humidity levels were achieved by controlling the N_2 flow rate. After adjusting the flow rate, we monitored for 10 min to allow the humidity level, the temperature, and the resonance frequency to stabilize. The resonance spectra of PEMS-2 at various relative humidity levels are shown in Fig. 3(a). Clearly, the resonance peak shifted to a higher (lower) frequency when the relative humidity was decreased (increased) due to the adsorption (desorption) of water molecules on the SiO_2 surface. In all experiments, the temperature was constant with less than 0.1 °C variations. In Fig. 3(b), we plot the resonance frequency of the third resonance peak of PEMS-1 and that of the first resonance peak of PEMS-2 versus the humidity where the full (open) symbols indicate humidity-increasing (decreasing) cycles. As can be seen the resonance frequency shift versus relative humidity was reversible and the data from both humidity-increasing and humidity-decreasing cycles collapsed in one single curve for each PEMS. For the relative humidity change from 60% to 30%, we obtained a −2400 Hz frequency shift with the third resonance peak of PEMS-1 and a −4600 Hz frequency shift with the first resonance peak of PEMS-2, corresponding to a sensitivity of 80 and 150 Hz frequency shift per percent humidity change for PEMS-1 and PEMS-2, respectively. To quantify the mass per unit area change due to the humidity change, a 10 MHz quartz crystal microbalance (QCM)[26] (Fortiming Co., Marlborough, MA) was also placed in the

Downloaded 25 Jul 2006 to 129.25.131.237. Redistribution subject to AIP license or copyright, see http://apl.aip.org/apl/copyright.jsp

humidity chamber. The present PEMS had a platinum surface on one side and a SiO_2 surface on the other. For close comparison, we sputtered (Denton II, Denton, Moorestown, NJ) platinum on one electrode of the QCM and coated silicon oxide on the other by spin coating 3-mercaptopropolsilane (MPS) (Alfa Aesar, Ward Hill, MA) followed by cross-linking at $p\mathrm{H}=11$.[27] For the same humidity change from 60% H to 30% H, the 10 MHz QCM exhibited a resonance frequency shift $\Delta f_{\mathrm{QCM}}=50$ Hz. Note that the 4600 Hz shift obtained with PEMS-2 was about two orders of magnitude larger than that obtained by the QCM and was also more than 20 times larger than the 170 Hz shift obtained by a ZnO PEMS with a humidity shift from the ambient humidity to saturation.[16] The mass change per unit area, Γ, can be deduced from Δf_{QCM} using the Sauerbrey equation,[26] $\Gamma=-\Delta f_{\mathrm{QCM}}\sqrt{\mu_q\rho_q}/2f^2$, where f is the natural resonance frequency of the QCM, $\mu_q=2.947\times10^{11}$ dyn/cm^2 and $\rho=2.648$ g/cm^3 are the shear modulus and density of the quartz, respectively. The Sauerbrey equation was valid in the present humidity range in that neither resonance peak intensity change nor deviation in the slope of the resonance frequency versus relative humidity in the QCM was observed in the humidity range of 30%–60%, indicating no appreciable viscosity effects for the QCM in this humidity range.[28,29] With $\Delta f_{\mathrm{QCM}}=50$ Hz $\Gamma=2.2\times10^{-7}$ g/cm^2 was obtained. With $\Delta m/\Delta f=\Gamma Lw/\Delta f$, we obtained $\Delta m/\Delta f=2\times10^{-14}$ and 1×10^{-15} g/Hz for the third resonance peak of PEMS-1 and the first resonance peak of PEMS-2, respectively, about four to five orders of magnitude more sensitive than the $\Delta m/\Delta f=8\times10^{-10}$ g/Hz for the 10 MHz QCM, three to four orders of magnitude more sensitive than ZnO-based PEMS,[14,15] and 100 times more sensitive than the existing PZT/Si_3N_4 PEMS (Refs. 8 and 9) for in-air detection applications. The improved sensitivity was in part attributed to the deduced cantilever size that contributed a factor of about 50 to the mass sensitivity improvement of PEMS-2 over that of the PZT/Si_3N_4 PEMS (Refs. 7–9) and an additional enhancement factor of about 1.5 due to the SiO_2 extension design of PEMS-2.[30]

In general, both mass changes and spring-constant changes can contribute to a cantilever's resonance frequency shift. For a uniformly distributed mass change Δm, over the entire cantilever surface, the mass sensitivity can be expressed as[18] $(\Delta m/\Delta f)_{\mathrm{mass}}=2M/f$ where M and f are the mass and resonance frequency of the PEMS, and the subscript "mass" denotes the mass-change effect only. With $M=3.3\times10^{-7}$ g for PEMS-1 and $M=2.5\times10^{-8}$ g for PEMS-2, we obtained $(\Delta m/\Delta f)_{\mathrm{mass}}=2.0\times10^{-12}$ g/Hz for the third resonance peak of PEMS-1 and 1.2×10^{-13} g/Hz for the first resonance peak of PEMS-2. Both were about 100 times less sensitive than the experimentally obtained values, indicating that mechanisms other than mass change were operating at this length scale. Similar 100-times mass sensitivity enhancements have also been observed in other PZT/Si_3N_4 PEMS,[7–9] and were attributed to the spring-constant change stresses.[7–9] It is of interest to find out at what cantilever size the crossover from the mass-loading regime to the adsorption-stress regime occurs.

This work is supported in part by the National Institute of Health (NIH) under Grant No. 1 R01 EB000720 and the Environmental Protection Agency (EPA) under Grant No. R82960401. This publication was supported by the Pennsylvania State University Nanofabrication Facility and the National Science Foundation Cooperative Agreement No. 0335765, National Nanotechnology Infrastructure Network, with Cornell University.

[1] J. Fritz, M. K. Baller, H. P. Lang, H. Rothuizen, P. Vettiger, E. Meyer, H.-J. Guntherodt, Ch. Gerber, and J. K. Gimzewski, Science **288**, 316 (2000).
[2] B. Ilic, D. Czaplewsli, H. G. Craighead, P. Neuzil, C. Campagnolo, and C. Batt, Appl. Phys. Lett. **77**, 450 (2000).
[3] T. Thundat, E. A. Wachter, S. L. Sharp, and R. J. Warmack, Appl. Phys. Lett. **66**, 1695 (1995).
[4] J. W. Yi, W. Y. Shih, R. Mutharasan, and W.-H. Shih, J. Appl. Phys. **93**, 619 (2003).
[5] W. Y. Shih, G. Campbell, J. W. Yi, R. Mutharasan, and W. H. Shih, in *Nanotechnology and the Environment: Applications and Implications*, edited by B. Karn, T. Masciangioli, W.-X. Zhang, V. Colvin, and P. Alivasatos (Oxford University Press, New York, 2004), Sec. 5.
[6] K. S. Hwang, J. H. Lee, J. Park, D. S. Yoon, J. H. Park, and T. S. Kim, Lab Chip **4**, 547 (2004).
[7] J. H. Lee, K. S. Hwanga, J. Park, K. H. Yoon, D. S. Yoon, and T. S. Kim, Biosens. Bioelectron. **20**, 2157 (2005).
[8] H. Yoon, K. H. Yoon, K. H. Park, J. Ahn, and S. Kim, Biosens. Bioelectron. **20**, 269 (2004).
[9] J. H. Lee, T. S. Kim, and K. H. Yoon, Appl. Phys. Lett. **84**, 3187 (2004).
[10] J.-P. McGovern, W. Y. Shih, and W.-H. Shih, Mater. Res. Soc. Symp. Proc. **845**, AA3.8.1 (2005).
[11] http://cfpub.epa.gov/ncer_abstracts/index.cfm/fuseaction/display.abstractDetail/abstract/2372/report/
[12] Q. Zhao, Q. Zhu, W. Y. Shih, and W.-H. Shih, Sens. Actuators B (in press).
[13] B. Rogers, L. Manning, M. Jones, T. Sulchek, K. Murray, B. Beneschott, J. D. Adams, Z. Hu, T. Thundat, H. Cavazos, and S. C. Minne, Rev. Sci. Instrum. **74**, 4899 (2003).
[14] L. A. Pinnaduwage, A. Wig, D. L. Hedden, A. Gehl, D. Yi, T. Thundat, and R. T. Lareau, J. Appl. Phys. **95**, 5871 (2004).
[15] L. A. Pinnaduwagea, T. Thundat, A. Gehla, S. D. Wilsona, D. L. Heddena, and R. T. Lareaub, Ultramicroscopy **100**, 211 (2004).
[16] J. D. Adams, G. Parrott, C. Bauer, T. Sant, L. Manning, M. Jones, B. Rogers, D. McCorkle, and T. L. Ferrell, Appl. Phys. Lett. **83**, 3428 (2003).
[17] B. Ilic, Y. Yang, K. Aubin, R. Reichenbach, S. Krylov, and H. G. Craighead, Nano Lett. **5**, 925 (2005).
[18] J. W. Yi, W. Y. Shih, and W.-H. Shih, J. Appl. Phys. **91** 1680 (2002).
[19] J. D. Adams, L. Manning, B. Rogers, M. Jones, and S. C. Minne, Sens. Actuators, A **121**, 262 (2005).
[20] C. Lee, T. Itoh, and T. Suga, Sens. Actuators, A **A72**, 179 (1999).
[21] D. Karanth and H. Fu, Phys. Rev. B **72**, 064116 (2005).
[22] H. Kueppers, T. Leuerer, U. Schnakenberg, W. Mokwa, M. Hoffmann, T. Schneller, U. Boettger, and R. Waser, Sens. Actuators, A **A97/A98**, 680 (2002).
[23] B. Piekarski, M. Dubey, E. Zakar, D. DeVoe, and D. Wickenden, Integr. Ferroelectr. **42**, 25 (2002).
[24] http://www.piezo.com/prodsheet2sq5H.html
[25] W. Y. Shih, and W.-H. Shih, in "Nanosensors for environmental applications," Series on Nanotechnology for Life Sciences Vol. 5: *Impact of Nanomaterials on Environment*, edited by C. Kumar (Wiley-VCH, Hoboken, 2006).
[26] G. Sauerbrey, Phys. Verh. **8**, 113 (1957).
[27] J. Bermudas, Master's thesis, Drexel University, 2005.
[28] H. Habuka, K. Suzuki, S. Okamura, M. Shimada, and K. Okuyama, J. Electrochem. Soc. **152**, G241 (2005).
[29] F. Pascal-Delannoy, B. Sorli, and A. Boyer, Sens. Actuators, A **A84**, 285 (2000).
[30] Z. Shen, W. Y. Shih, and W.-H. Shih, Rev. Sci. Instrum. **77**, 065101 (2006).

Downloaded 25 Jul 2006 to 129.25.131.237. Redistribution subject to AIP license or copyright, see http://apl.aip.org/apl/copyright.jsp